Violation of detailed balance in microwave circuits: theory and experiment

Alexandre Dumont,[1] Pierre Février,[1] Christian Lupien,[1] and Bertrand Reulet[1]

[1] *Département de physique and Institut Quantique, Université de Sherbrooke, Sherbrooke, Québec, J1K 2R1, Canada.*

(Dated: May 5, 2023)

We propose a new approach to detailed balance violation in electrical circuits by relying on the scattering matrix formalism commonly used in microwave electronics. This allows to include retardation effects which are paramount at high frequencies. We define the spectral densities of phase space angular momentum, heat transfer and cross power, which can serve as criteria for detailed balance violation. We confirm our theory with measurements in the 4-8 GHz frequency range on several two port circuits of varying symmetries, in space and time. This validates our approach, which allows to treat quantum circuits at ultra-low temperature.

I. INTRODUCTION

There has been recently a fast growing interest in the thermodynamics of ultimately simple, small systems, in particular through the study of heat engines [1–4] or particles driven by noise sources [5], such as brownian motion in a fluid [6]. A particular effort has been devoted to electrical circuits, in which the variables such as position or velocity of the brownian particle are replaced by macroscopic variables in the circuit, such as charge or voltage across a capacitor, and where the noise is the Johnson-Nyquist thermal noise of resistors [7–9]. All these systems, from biological entities to electrical circuits, may indeed obey similar equations of motion.

The simplest and most intensively studied circuit consists of two capacitors coupled to two resistors through another capacitor. Even such a simple circuit shows nontrivial heat transport [10–13], gyration and detailed balance violation [8, 9]. Most of these studies have been performed within the framework of classical physics. On the other hand there is a currently huge development of quantum technologies and circuits, understanding the thermodynamical properties of which is of utmost interest. It is thus crucial to extend the methods developed in classical circuits to quantum ones. [14]

A mandatory condition to study circuits in the quantum regime is to work at frequencies, f, such that $hf \gtrsim k_BT$ with T the temperature. Since a temperature $T = 1$K corresponds to a frequency $f = k_BT/h = 21$ GHz, experiments are usually performed below 1K in the microwave domain. Since circuits are usually larger than the wavelength, retardation effects are paramount. Unfortunately, previous studies in classical circuits have focused to low frequencies where retardation effects are irrelevant and were not considered. It is the goal of the present paper to provide a new theoretical approach, based on the scattering matrix formalism, able to treat the case of circuits of any size and to validate the theory with experiments in the microwave regime.

The rest of the paper will be structured as follows: section II is the theory, where we introduce the scattering matrix formalism and express the metrics for detailed balance violation in terms of it. Section III goes over the experimental setup used to test our theoretical predictions in the microwave regime. Section IV presents the experimental data while we conclude in section V.

II. THEORY

Detailed balance refers to the absence of probability currents in phase space. It can be demonstrated using global metrics such as heat current or angular momentum in phase space. Previous work has focused on circuits without propagation, modeling them using time-domain differential equations between current and voltages in the circuit, and where noise sources appear as source terms [8, 9]. Below we derive expressions for these quantities when the system is described by a scattering matrix in frequency domain.

A. Scattering matrix formalism

We consider linear circuits where current and voltages are simply related by a frequency-dependent impedance matrix. Measuring voltages (respectively currents) requires high impedance (respectively low impedance) sensors, which are difficult to implement at high frequency. One would rather work with matched amplifiers, i.e. amplifiers which input impedance is the same as that of the transmission line connected to it, so that all the power sent to the amplifier is absorbed. Such amplifiers do not measure the voltage at a point in the circuit but the amplitude of the wave incoming to it. We will focus on matched amplifiers and discuss briefly the case of voltmeters. We chose to work, as usual in microwave electronics, with the scattering formalism [15]. In this formalism, a circuit connected to n ports is modeled by a $n \times n$ matrix, the scattering matrix S, which relates the amplitude of the voltage waves exiting each port to that entering each port. Sources appear as incoming waves and measurements can be performed on each outgoing wave.

In the following we will apply the scattering formalism to the simplest, yet nontrivial circuit, which contains

only two ports, i.e. two noise sources and two measurements, as shown in Fig. 1. This situation is very close to the one usually considered at low frequency [8–11]. This is the setup we have implemented experimentally, as we show below. More complex circuits can be easily treated following the same lines. We suppose that the circuit is lossless and linear. Losses can be implemented by adding extra ports in which power exits the circuit. According to the fluctuation-dissipation theorem, losses must be accompanied by noise, i.e. extra noise sources must be added accordingly, which enter the circuit through the extra ports. Non-linearities would complexify the physics a lot, since different frequencies would be coupled, and the usual scattering formalism does not apply to such systems. We do not consider non-linearities, so voltage measured at a given frequency depends only on noise sources at the same frequency. As a consequence, we can deal with the spectral densities of the various quantities we are considering, and not necessarily their integral over a certain bandwidth.

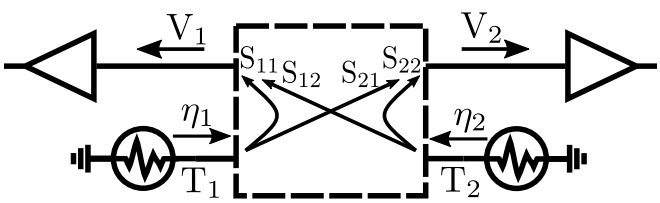

Figure 1. **(a)** Two matched resistors of value R_0 at temperatures T_1 and T_2 and emitting voltage noises η_1 and η_2 respectively. Both noises act as inputs into a 2 port circuit represented by its four scattering parameters, while V_1 and V_2 correspond to the measured outputs.

Following Fig. 1 we note $\eta_1(f)$ and $\eta_2(f)$ the voltage amplitude of the waves emitted by the noise sources at frequency f, and $V_1(f)$, $V_2(f)$ the measured amplitudes of the waves leaving the circuit. They are related by:

$$V_1(f) = S_{11}(f)\eta_1(f) + S_{12}(f)\eta_2(f), \quad (1)$$
$$V_2(f) = S_{21}(f)\eta_1(f) + S_{22}(f)\eta_2(f), \quad (2)$$

where S_{ij} are the frequency-dependent elements of the S matrix. For the sake of simplicity we suppose that the noise sources are uncorrelated and of spectral density $\left\langle |\eta_i(f)|^2 \right\rangle = k_B T_i R_0$. Here R_0 is the impedance of the sources, which are matched to the transmission lines connecting to the two ports of the circuit (for simplicity we take the same R_0 for both sources). T_i is the (possibly frequency-dependent) noise temperature of the source i. If the noise sources are resistors in the classical regime, T_i is simply their thermodynamic temperature [16, 17]. If they are resistors in the quantum regime, the noise temperature T_i is related to the thermodynamical temperature $\mathcal{T}$ by $T_i(f) = (hf/2k_B)\coth(hf/2k_B\mathcal{T}))$.

Below we focus on two questions: i) how to compute interesting physical quantities introduced in previous work, such as heat transfers and fluctuations loops [8], using our approach? ii) can one find a better way to determine if the circuit is out of equilibrium?

B. Heat transfers

A lot of work has been devoted to the heat transfer between two capacitively coupled resistors [10–13]. Similar quantities can be calculated using the scattering formalism. Following [10] we note $\dot{Q}_1$ the electrical power dissipated in the resistor at port 1. Since this quantity is nonlinear in voltage, it mixes frequencies: its spectral density involves a convolution in frequency space. However the spectral density of average power $\langle \dot{q}_1(f) \rangle$ is well defined, given by:

$$\langle \dot{q}_1(f) \rangle = \frac{1}{R_0}\left[\left\langle |V_1(f)|^2 \right\rangle - \left\langle |\eta_1(f)|^2 \right\rangle\right] \quad (3)$$

This has a clear interpretation: it corresponds to cooling the resistor by emission of a wave of amplitude η_1 and heating by the absorption of a wave of amplitude V_1. It corresponds to the net power transfer from the left part of Fig.1 into the circuit. Introducing the detected power spectral densities $p_i = \left\langle |V_i|^2 \right\rangle / R_0$ and their difference by $\Delta p = p_1 - p_2$, we find:

$$\langle \dot{q}_1 \rangle = \frac{|S_{12}|^2}{2|S_{12}|^2 - 1}\Delta p. \quad (4)$$

This result is a generalization of what has been obtained at low frequency, see Eq. (16) of ref. [7]. Thus Δp is a measure of the heat current, which vanishes at equilibrium. This also means that for any circuit, there cannot be a difference between the two power spectral densities detected unless $\Delta T = T_1 - T_2 \neq 0$, provided that $|S_{12}|^2 \neq 1/2$, i.e. the circuit must not divide power equally, in which case Δp always vanishes.

C. Angular momentum and stochastic area

It was demonstrated in [8, 9] that fluctuation loops are observed in out of equilibrium circuits. These loops are closed trajectories in the (V_1,V_2) plane, characterized by a stochastic area A. The existence of fluctuation loops corresponds to an average rotation of (V_1, V_2) to which is associated an angular momentum along the perpendicular axis given by:

$$\langle L_z \rangle = \left\langle V_1(t)\dot{V}_2(t) - V_2(t)\dot{V}_1(t) \right\rangle \quad (5)$$

It is simply related to the stochastic area by $\langle L_z \rangle = 2\left\langle \dot{A} \right\rangle$. This reads in Fourier space:

$$\langle L_z \rangle = \int_{-\infty}^{+\infty} \langle l_z(f) \rangle \, df. \tag{6}$$

with $\langle l_z(f) \rangle$ the angular momentum spectral density. Experimentally the integral will have finite bounds due to the finite bandwidth of the circuit. We find:

$$\langle l_z(f) \rangle = 4\pi f \, \mathrm{Im}\left[\langle V_1(f) V_2^*(f) \rangle\right]. \tag{7}$$

Thus the cross-correlation between V_1 and V_2 is a measure of the angular momentum, which vanishes at equilibrium. Indeed, we find: $\langle V_1(f) V_2^*(f) \rangle / R_0 = \beta k_B \Delta T$ with $\beta = S_{11} S_{21}^*$. This means that for any circuit, there cannot be any correlation between the two voltages detected, unless $\Delta T \neq 0$. The only condition is $\beta \neq 0$, i.e. the circuit must have a finite transmission. The condition on the angular momentum is however more stringent because of the imaginary part: if β is real then $\langle l_z \rangle = 0$. This remark sheds light on the simple reason why there are loops: the circuit must introduce a phase difference between the two branches, so that for each frequency, the two noise sources generate a rotating point in the (V_1, V_2) plane. Because of the unitarity of the S matrix the two rotate in opposite directions, and if the amplitude of the two noise sources are equal, there is no global rotation. The overall direction of rotation depends on the sign of ΔT as well as the sign of the phases in the S matrix.

D. Cross Power

The difference in auto-correlations and the cross-correlation of the detected voltage can be used to detect deviation from equilibrium. Experimentally these two quantities can be affected by imperfections: the first is sensitive to asymmetries in the detection (amplitude mismatch) and amplifier noise, while the second is sensitive to to phase mismatch due e.g. to difference in cable lengths. The angular momentum appears to be related to the cross-correlation $\langle V_1 V_2^* \rangle$ via one of it's quadrature, and with a weighing factor f. It is clear that neither the absolute phase of $\langle V_1 V_2^* \rangle$ nor the frequency-dependent weighing factor are essential to determine if the circuit is out of equilibrium. Thus on a practical point of view it might be interesting to define the cross correlation power spectral density as

$$\langle p_{1,2} \rangle = \frac{1}{R_0} |\langle V_1 V_2^* \rangle|, \tag{8}$$

where we take the modulus of the cross correlation to remove the phase problem. This quantity is also a good metric of ΔT that is immune to amplifier noise and cable lengths. However it does not allow to know which source is hotter than the other.

III. EXPERIMENTAL SETUP

We have performed a thorough experimental test of our theoretical results. Beyond checking the formulas, the goal was to demonstrate the following prediction that emerges from our calculations: breaking spatial and/or time reversal symmetries cannot generate heat current or angular momentum, only ΔT matters. For this we performed measurements on circuits with various symmetries, see bottom of Fig.2. Note that while spatial symmetry has been already considered in previous work, time-reversal symmetry could not be probed since propagation times were neglected.

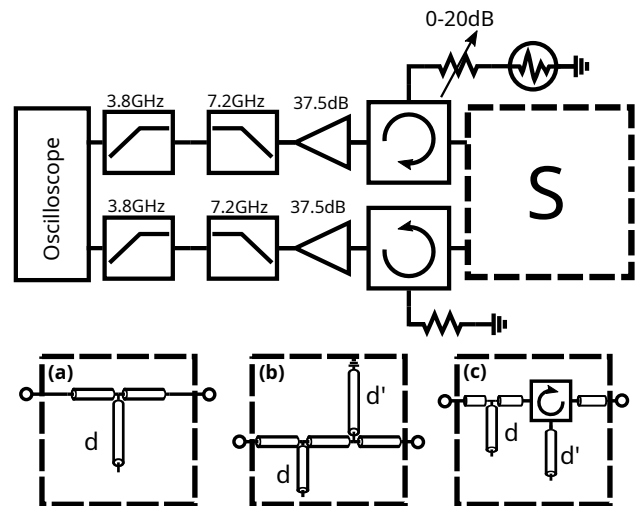

Figure 2. (Top) Experimental setup. The dashed box represents the coupling circuit of scattering matrix S. (Bottom) All three coupling circuits used to test different S matrices.

The experimental setup is shown on Fig. 2. All measurements have been performed at room temperature using a variable attenuator and a calibrated noise source as the hot source (T_1 adjustable between 290K and 560K) and a 50Ω resistor at room temperature as the cold source ($T_2 = 290$K). We have chosen to work in the 4-8 GHz frequency range, which is similar to that of many experiments performed in the quantum regime at ultra low temperature. The separation between incoming and outgoing waves is achieved using two circulators: the signals emitted by the sources are injected in the circuit and not in the related amplifiers, while those leaving the circuits enter the amplifiers and are not lost in the sources. Moreover, the noise emitted by the amplifiers is absorbed by the sources which are matched to the microwave circuit. This minimizes parasitic cross-correlations. Given the noise temperature ~ 70K of the amplifiers and isolation of the circulators, we estimate a parasitic contribution of ~ 0.7K (more circulators could be used if needed). After amplification and filtering to keep the signal within a well defined bandwidth, the signals are digitized using a 20GHz, 40GS/s, 8 bit digital oscilloscope. The time series are acquired in batches of 2MS that are split in

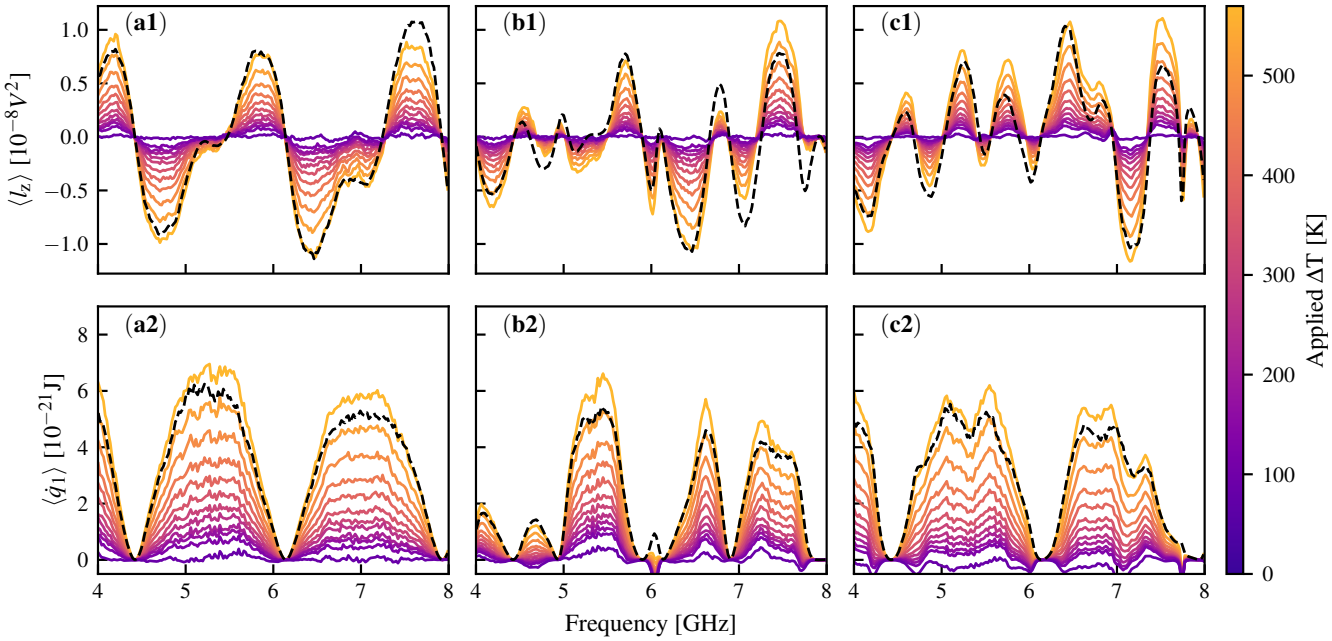

Figure 3. (a1) [resp. (b1), (c1)]: Measured average spectral density of angular momentum for the circuit of Fig. 2(a) [resp. (b), (c)] as a function of frequency in the 4-8 GHz range. Different colors correspond to different temperature differences according to the color bar on the right. The dashed lines represent the prediction of Eq.(7) using the measured scattering parameters and $\Delta T = 570$K. It is thus proportional to $f\,\mathrm{Im}\,[S_{12}S_{22}^*]$. (a2) [resp. (b2), (c2)]: Measured average power spectral density for the circuit of Fig. 2(a) [resp. (b), (c)] as a function of frequency in the 4-8 GHz range. Different colors correspond to different temperature differences according to the color bar on the right. The dashed lines represent the prediction of Eq.(4) using the measured scattering parameters and $\Delta T = 570$K. It is thus proportional to $|S_{12}|^2$.

chunks of 2048 points. Spectra are then calculated using a discrete Fourier transform on each chunk. Then we calculated the auto- and cross-correlations using those spectra and averaged over all the chunks. The size of the chunk sets the frequency resolution, here 20MHz, which is enough for the circuits we considered.

In order to test the effect of spatial/time reversal symmetries, we have studied the three circuits shown in Fig. 2. The circuits are made of pieces of coax cables of various lengths connected by T-junctions, and terminated by open or short circuits. The lengths d, d' of 5.08 and 7.62 cm respectively, where chosen so that reflections of waves at the end of the cables and at the junctions provide rich interference patterns which result in strong frequency-dependence of the S-matrix, thus providing a deep test of our theoretical results, see dashed lines in Fig. 3. Here propagation times are essentials. Circuit (a) in Fig. 2 is symmetric upon exchange of ports 1 and 2 while circuit (b) is not. Circuit (c) contains a circulator in order to break time-reversal symmetry. In order to make a quantitative comparison between our predictions and the measurements, we have measured the S matrix of all three circuits using a vector network analyzer (VNA), see dashed lines in Fig. 3.

IV. RESULTS

In Fig. 3 we show the spectral densities of the angular momentum $\langle l_z(f)\rangle$ (top) and transferred power $\langle \dot{q}_1(f)\rangle$ (bottom) as a function of frequency for the three circuits of Fig. 2. The two quantities exhibit strong oscillations vs. frequency which come from interferences occurring due to total reflections at the end of the cables and partial reflections at the junctions between them. We observe a very good quantitative agreement between the measurements and theoretical predictions of Eqs. (7) and (4), shown as dashed lines in Fig. 3. These have been obtained using the measured coefficients of the scattering matrix and the calibrated noise temperature of the hot noise source. We attribute the small differences between theory and experiment to experimental imperfections, in particular the lack of reproducibility of connections/disconnections between the VNA and noise measurements, and the losses in the cables and circulator. The slightly negative values of $\langle \dot{q}_1\rangle$ are due to the presence of amplifier noise which is not accounted for in Eq. (4).

The dependence of the integrated angular momentum $\langle L_z\rangle$ and cross-power $\langle P_{1,2}\rangle$ on the temperature difference ΔT is shown in Fig. 4. These curves have been obtained by integrating the spectra of Fig. 3 over frequency between 7.3 and 7.5 GHz for the angular momentum and

the full 4-8 GHz bandwidth for the cross power (the relatively narrow bandwidth for $\langle l_z(f)\rangle$ has been chosen to avoid sign change leading to a vanishing $\langle L_z\rangle$). The data corresponding to $\Delta T < 0$ have been obtained by swapping the cold and hot sources. As predicted, $\langle L_z\rangle \propto \Delta T$, and $\langle P_{1,2}\rangle \propto |\Delta T|$. This is true for all circuits, i.e. is independent of the presence or absence of spatial and/or time-reversal symmetries in the system.

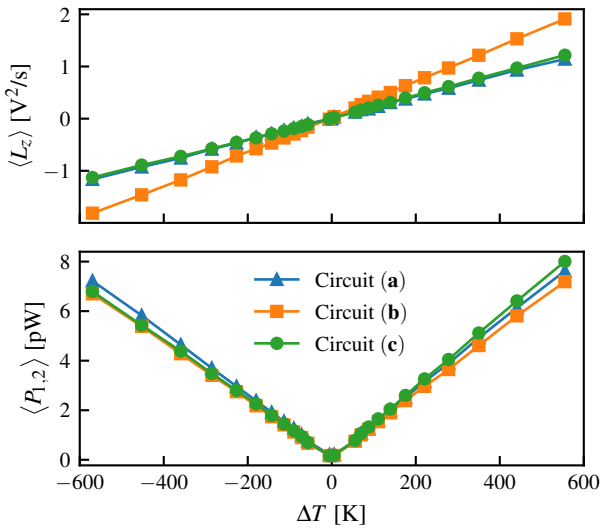

Figure 4. (Top) Total angular momentum in the frequency range 7.3−7.5 GHz for the three circuits of Fig. 2 as a function of ΔT. (Bottom) Total cross-power in the frequency range $4-8$ GHz for the three circuits of Fig. 2 as a function of ΔT.

We notice that $\langle P_{1,2}\rangle$, which in theory should be proportional to $|\Delta T|$ is experimentally not exactly a perfectly even function of ΔT. This comes from the impedances of the sources not being exactly 50 Ω, so reversing the sources also slightly changes S. The same thing happens to $\langle L_z\rangle$ which is not perfectly odd, although it is less obvious. For $\Delta T = 0$ we find a residual cross-power which corresponds to what we expect for $\Delta T \sim 13$K. We understand this as amplifier noise ($\sim$ 70K) being averaged a finite number $N = 100$ of times. This yields $\Delta T \approx 70/\sqrt{100} = 7$K, in reasonable agreement with the measurement. We also find a residual angular momentum corresponding to $\Delta T \sim 0.6$K, in good agreement with our prediction, see section III.

V. CONCLUSION

We have shown, both theoretically and experimentally how heat transfer and angular momentum, quantities that have been introduced in electrical circuits at low frequency in the context of detailed balance violation, can be extended to microwave circuits where propagation delays are paramount. Our approach is very general and could be used not only for microwaves but also for guided optics for example. In particular, it allows to treat circuits in the quantum regime ($hf \gtrsim k_{\rm B}T$) where the noise spectra of the sources have a frequency dependence which reflects the presence of vacuum fluctuations[12].

From our result one should be able to recover previously obtained results at low frequency where propagation times vanish [10, 11]. For this we have to consider voltmeters and not only matched amplifiers as we did. This can be done as follows: a voltmeter does not measure the outgoing voltage V_{out} but the sum of the incoming V_{in} and outgoing voltages, $V_{in} + V_{out}$. As a consequence, our approach is valid provided we replace the scattering matrix S by $S+1$. However, the latter matrix being non-unitary, simplifications of the formula cannot be carried out.

We have focused on the detection of detailed balance violation using average quantities: average heat transfer, average angular momentum. These involve the measurement of the second order correlations of the detected voltages. Some previous works have considered fluctuations of these quantities and calculated their probability distribution [10–12]. With our approach, it is possible to reconstruct these distributions by measuring their moments. For example, the variance of the angular momentum is related to correlations of order 4 of the measured voltages. Dealing with moments would be interesting in particular with non-gaussian noise: what happens in a circuit with two noise sources of equal variance but opposite third moments, generated for example by two shot noise sources with opposite bias ?

ACKNOWLEDGEMENTS

The authors would like to acknowledge the many conversations with Clovis Farley and Simon Bolduc Beaudoin. This work was supported by the Canada Research Chair program, the NSERC, the Canada First Research Excellence Fund, the FRQNT, and the Canada Foundation for Innovation.

[1] R. Filliger and P. Reimann, Brownian Gyrator: A Minimal Heat Engine on the Nanoscale, Physical Review Letters **99**, 230602 (2007).

[2] A. Argun, J. Soni, L. Dabelow, S. Bo, G. Pesce, R. Eichhorn, and G. Volpe, Experimental Realization of a Minimal Microscopic Heat Engine, Physical Review E **96**, 052106 (2017).

[3] H. C. Fogedby and A. Imparato, Autonomous Quantum Rotator, EPL (Europhysics Letters) **122**, 10006 (2018).

[4] I. Sou, Y. Hosaka, K. Yasuda, and S. Komura, Nonequilibrium probability flux of a thermally driven micromachine, Physical Review E **100**, 022607 (2019).

[5] W. A. M. Morgado and T. Guerreiro, A study on the action of non-Gaussian noise on a Brownian particle, Physica A: Statistical Mechanics and its Applications **391**, 3816 (2012).

[6] I. A. Martínez, É. Roldán, L. Dinis, D. Petrov, J. M. R. Parrondo, and R. A. Rica, Brownian Carnot engine, Nature Physics **12**, 67 (2016), number: 1 Publisher: Nature Publishing Group.

[7] K.-H. Chiang, C.-L. Lee, P.-Y. Lai, and Y.-F. Chen, Electrical Autonomous Brownian Gyrator, Physical Review E **96**, 10.1103/PhysRevE.96.032123 (2017).

[8] A. Ghanta, J. C. Neu, and S. Teitsworth, Fluctuation Loops in Noise-Driven Linear Dynamical Systems, Physical Review E **95**, 032128 (2017).

[9] J. P. Gonzalez, J. C. Neu, and S. W. Teitsworth, Experimental metrics for detection of detailed balance violation, Physical Review E **99**, 022143 (2019), publisher: American Physical Society.

[10] S. Ciliberto, A. Imparato, A. Naert, and M. Tanase, Heat Flux and Entropy Produced by Thermal Fluctuations, Physical Review Letters **110**, 180601 (2013), publisher: American Physical Society.

[11] S. Ciliberto, A. Imparato, A. Naert, and M. Tanase, Statistical Properties of the Energy Exchanged between Two Heat Baths Coupled by Thermal Fluctuations, Journal of Statistical Mechanics Theory and Experiment , P12014 (2013).

[12] D. S. Golubev and J. P. Pekola, Statistics of Heat Exchange between Two Resistors, Physical Review B **92**, 085412 (2015).

[13] M. Baiesi, S. Ciliberto, G. Falasco, and C. Yolcu, Thermal Response of Nonequilibrium RC Circuits, Physical Review E **94**, 022144 (2016), publisher: American Physical Society.

[14] B. Bhandari, P. T. Alonso, F. Taddei, F. von Oppen, R. Fazio, and L. Arrachea, Geometric properties of adiabatic quantum thermal machines, Physical Review B **102**, 155407 (2020), publisher: American Physical Society.

[15] D. Pozar, *Microwave Engineering, 4th Edition* (Wiley, 2011).

[16] J. B. Johnson, Thermal Agitation of Electricity in Conductors, Physical Review **32**, 97 (1928), publisher: American Physical Society.

[17] H. Nyquist, Thermal Agitation of Electric Charge in Conductors, Physical Review **32**, 110 (1928), publisher: American Physical Society.